A Three-Dimensional Model of a DC Thermal Plasma Torch for Waste Treatment Applications

N.Y. Mendoza Gonzalez[1], L. Rao[2], P. Carabin[2], A. Kaldas[2], J.L. Meunier[1]

[1]*Department of Chemical Engineering, McGill University, Montreal, Canada*
[2]*PyroGenesis Canada Inc., Montreal, Canada*

Abstract:

A three-dimensional (3-D) turbulent model of a Direct Current (DC) plasma torch is presented to analyze the arc behavior under different conditions. The model includes the simultaneous solution of conservation of mass, momentum, energy and electromagnetism equations. A parametric study is performed by varying the air injection rate by a factor of 16:1. The results aim to provide a better understanding and control of the anode erosion process.

Keywords: DC plasma torch, modeling, electric arc, anode erosion.

1. Introduction

Thermal plasma technology is being used successfully for waste treatment applications, allowing the conversion of wastes into clean energy while producing no secondary residue. The extreme temperatures generated by plasma torches (5,000 to 10,000 degrees Celsius, depending on the type of plasma forming gas used) allows for highly efficient gasification reactors, requiring small volumes [1]. Erosion of electrodes remains one important problem in the direct current (DC) plasma torches used in waste treatment plants. Some of the factors viewed as important for controlling the erosion rates are the arc current, the arc root mobility, the plasma gases used, and the nature of the electrode material itself. Certainly, electrode erosion is directly related to the arc behavior inside the torch. This work presents a 3-D turbulent model aimed at predicting the arc behavior inside the torch under different operating conditions and provides some design guidelines for reducing anode erosion.

2. Plasma Model

The DC plasma torch studied includes a thermionic emitter cathode and a water-cooled tubular anode where the arc root attaches. The torch design includes a vortex of plasma forming gas injected between the two electrodes. This physical system is described by a system of mathematical equations that include the equations of continuity, energy, momentum and electromagnetic fields. The effects of turbulence mainly resulting from the vortex injection are taken into account by using the k-ε model.

A three-dimensional geometry is constructed and calculated in order to provide insight on the azimuthally asymmetric flow pattern from the gas vortex, from the localized arc root attachment and the resulting self setting arc length on the tubular anode. FLUENT™ 6.3 code is used as a modeling tool by implementing user defined functions (UDF) treating the phenomena related to plasma (plasma chemistry and electromagnetism). The following assumptions are used in the present model [2]:

- Global electrical neutrality;
- No account is taken of the electrode sheaths;
- Air plasma at local thermodynamic equilibrium (LTE);
- Optically thin plasma (e.g. use of a net emission coefficient);
- Steady state turbulent flow neglecting gravity effects.

These assumptions lead to the simplification of the conservation equations for momentum, heat and electromagnetic fields:

$$\frac{\partial}{\partial x}(\rho v_x)+\frac{\partial}{\partial y}(\rho v_y)\frac{\partial}{\partial z}(\rho v_z)=0 \tag{1}$$

$$\begin{aligned}&\frac{\partial}{\partial x}(\rho v_z v_x)+\frac{\partial}{\partial y}(\rho v_z v_y)+\frac{\partial}{\partial y}(\rho v_z v_z)=-\frac{\partial p}{\partial z}\\&+\frac{\partial}{\partial x}\left[-\mu\left(\frac{\partial v_z}{\partial x}+\frac{\partial v_x}{\partial z}\right)\right]+\frac{\partial}{\partial y}\left[-\mu\left(\frac{\partial v_y}{\partial z}+\frac{\partial v_z}{\partial y}\right)\right]\\&+\frac{\partial}{\partial z}\left[-\mu\left(2\frac{\partial v_z}{\partial z}-\frac{2}{3}+(\vec{\nabla}\cdot\vec{v})\right)\right]+S_{v_z}\end{aligned} \tag{2}$$

$$\begin{aligned}&\frac{\partial}{\partial x}(v_x(\rho E+p))+\frac{\partial}{\partial y}(v_y(\rho E+p))+\frac{\partial}{\partial z}(v_z(\rho E+p))\\&=\frac{\partial}{\partial x}\left(k\frac{\partial T}{\partial x}\right)+\frac{\partial}{\partial y}\left(k\frac{\partial T}{\partial y}\right)+\frac{\partial}{\partial z}\left(k\frac{\partial T}{\partial z}\right)+S_E\end{aligned} \tag{3}$$

Where, ρ, μ and k are respectively the density, the viscosity and the thermal conductivity of the plasma gas. The Lorentz forces $\vec{F} = \vec{J} \times \vec{B}$, the Joule heating and the source terms (S_{vz} and S_E) in the Navier–Stokes equations are the link between fluid mechanics and electromagnetic fields inside the plasma stream.

For the electromagnetic conservation equations, the variables to solve are the electrical scalar potential φ and the electrical vector potential $\vec{A}$. Knowing $\vec{A}$ enables the calculation of the magnetic field $\vec{B}$ since they are related through the relationship $\vec{\nabla} \times \vec{B} = \vec{A}$. No external magnetic field is imposed on the system. The scalar potential equation is as follows:

$$\frac{\partial}{\partial x}\left(\sigma \frac{\partial \varphi}{\partial x}\right) + \frac{\partial}{\partial y}\left(\sigma \frac{\partial \varphi}{\partial x}\right) + \frac{\partial}{\partial z}\left(\sigma \frac{\partial \varphi}{\partial x}\right) = 0 \qquad (4)$$

Where, σ is the electrical conductivity. Finally, the vector potential component is represented by:

$$-\vec{\nabla}^2 \cdot A_x = \mu_0 J_x \qquad (5)$$

$$-\vec{\nabla}^2 \cdot A_y = \mu_0 J_y \qquad (6)$$

$$-\vec{\nabla}^2 \cdot A_z = \mu_0 J_z \qquad (7)$$

All the preceding conservation equations are elliptical partial differential equations (PDE) solved using the sequential solver of the CFD finite-volumes FLUENT^{TM} 6.3 [3]. The thermodynamic and transport properties within the system vary greatly and so are highly non-linear with temperature, especially in plasma. These dependencies are considered locally to assess the structure of fluids and fields of energy in the system. The properties for the air plasma gas are taken from [4]. The net emission coefficient is a simplified radiative transfer method that has proven quite effective for the case of thermal plasmas, where line emission is extremely significant when compared to flames. The method of net emission coefficient uses a simplified geometry (cylindrical homogeneous column of plasma) and a detailed description of the spectral lines. For each line, an escape factor representing the fraction of photons leaving the plasma column is calculated, and the total radiated power is obtained. Even if this method appears quite simplified, it estimates the radiative losses of thermal plasmas very well (radiation energy loss rate in J/(s m^3)). A net emission coefficient with a 5mm radius approximately corresponds to the size of the emissive thermal plasma arc column.

The boundary conditions are described in table (1), where P_{iN2} is 5% higher than P_{iair}.

Table 1 - Boundary conditions

($\gamma \equiv \partial\Omega / \partial\vec{n} = 0$, where Ω is the generic variable)

Variable	***p (Pa)***	$\vec{v}$ **(m/s)**	***T*** ***(K)***	φ **(V)**	$\vec{A}$ **(Wb/m)**
Inlet N_2	P_{iN2}	v_{in}	300	γ	γ
Inlet Air	P_{iair}	v_{in}	300	γ	γ
Cathode	γ	0	500	γ	γ
Cathode tip		0	500	$-\sigma\partial\varphi/\partial z = I/A$	γ
Outlet	γ	γ	γ	γ	γ
Anode	-	0	γ	0	γ

The mesh, which contains close to 357,000 cells, is based on PyroGenesis Canada Inc's design. It represents the cathode, nozzle, the vortex injection and the anode (Figure 1).

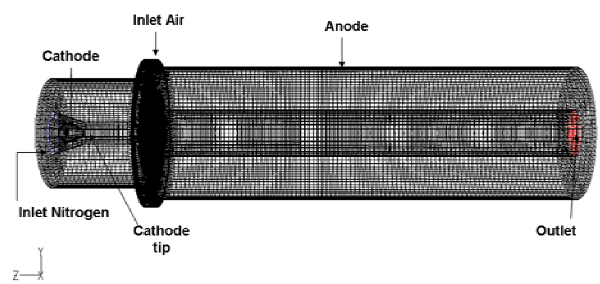

Fig.1 Mesh of the Torch.

3. Results

Preliminary modeling results allow for estimating the influence of the gas vortex injection on the fluid flow. Four cases are presented with normalized air flow rates of 0.0625, 0.25, 0.5 and 1 NSLPM which are named cases A, B, C and D respectively. The total power used for these calculations is 130 kW. Figure 2 shows this parametric study varying the air vortex injection and its effect on the axial velocity close to the anode wall. All curves are normalized to the overall maximum speed attained.

From Figure 2 it is observed that higher gas velocities yield higher vortex speeds, which correspond to lower anode erosion as seen experimentally. These high and radially symmetric velocities are responsible for maintaining the arc at the center of the tubular electrode until a reduction of the azimuthal velocities occurs and the arc attaches to the anode. For all cases studied, there is a velocity jump at the beginning of the anode. This jump is more important when injection rates are high as in cases C and D, while for cases A and B the jump is less important and velocity remains more stable throughout the anode wall.

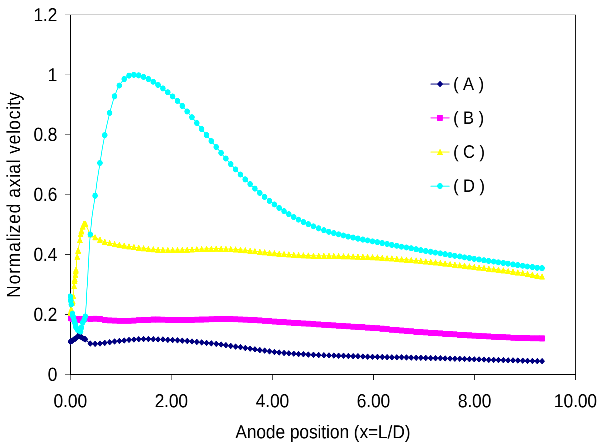

Fig. 2 Axial velocity distribution along the anode position (3 mm before the anode wall).

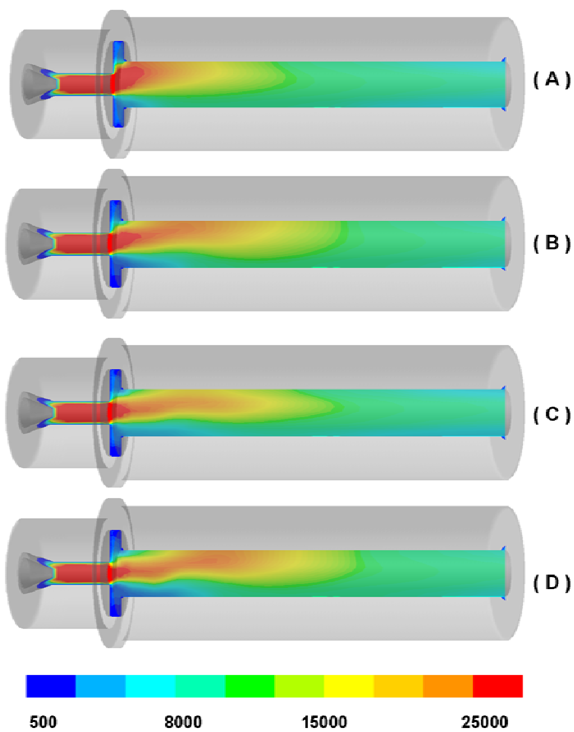

Fig. 3 Temperature contours [K] showing the arc root attachment for the different cases.

Figure 3 shows the temperature contours for the different air injection rates. The plasma model shows the very high temperature zone close to the cathode tip. This high temperature (25 000 K) is caused by the heat dissipation from the resistance of the plasma to the flow of electric current. In Figure 3, one can observe that the high intensity arc is being deflected before reaching the anode wall because of the vortex injection. The vortex injection stabilizes the arc column that is confined to the center of the tube. Centrifugal forces drive the cold fluid toward the walls of the arc chamber, which is thus thermally well protected. The intense convective cooling of the arc fringes from the vortex flow enhances the power dissipation per unit length of the arc column which, in turn, results in higher axis temperatures.

From Figure 3, it is seen that the free burning arc covers a larger surface area of the anode when injection rates are low. The effect of increasing the injection rate produces a downstream shift of the arc attachment on the anode. The arc attachment root covers an important area of the anode representing the area where it is expected that the most important erosion takes place. It is also observed that temperature remains high (around 10 000 K) at the exit of the anode, forming the plasma jet which will be used for downstream processing.

The size and shape of the arc attachment on the electrodes is very important in electrode erosion studies.. We can see here the positions and typical sizes of this arc attachment and the effect of increasing the vortex injection rate on these parameters. These results can be correlated to arc ablation traces in actual devices.

4. Conclusions

A 3-D DC arc model was developed in order to study the influence of the air injection rate on the arc column in a plasma torch. It is observed that higher gas velocities yield higher vortex speeds, which correspond to an arc root attachment pushed downstream on the anode surface. This should favor lower anode erosion because of a better distribution of the heat flux on the anode wall. Such phenomena as well as the gas injection scheme in thermal plasma torches require 3-D modeling to fully understand the flow, energy and electrodynamic fields. This modeling work is continuing to further understand and predict improved electrodes longevities.

References

[1] Heberlein and A. B. Murphy, “Thermal Plasma Waste Treatment”, J. Phys. D: Appl. Phys. 41, 053001 (20pp) (2008).

[2] A. Blais, P. Proulx and M. I. Boulos, "Three - dimensional numerical modelling of a magnetically deflected dc transferred arc in argon", J. Phys. D: Appl. Phys. 36, p. 488-496, (2003).

[3] Fluent’s Guide. Fluent 6.3 User-Defined Functions User’s Guide (Lebanon, NH) (2008).

[4] M.I. Boulos, P. Fauchais and E. Pfender, "Thermal Plasmas, Fundamentals and Applications" vol. 1 (New York: Plenum) (1994).